EMULSION TEMPLATED CROSSLINKED FIBROUS MEMBRANES *via* NEAR-GEL RESIN ELECTROSPINNING

PRAMOD MANIKANT GURAVE

DEPARTMENT OF TEXTILE AND FIBRE ENGINEERING

INDIAN INSTITUTE OF TECHNOLOGY DELHI

July 2024

EMULSION TEMPLATED CROSSLINKED FIBROUS MEMBRANES *via* NEAR-GEL RESIN ELECTROSPINNING

by

PRAMOD MANIKANT GURAVE

Department of Textile and Fibre Engineering

Submitted

in fulfilment of the requirements of the degree of Doctor of Philosophy

to the

INDIAN INSTITUTE OF TECHNOLOGY DELHI

July 2024

॥ राष्ट्र देवो भवः ॥

Dedicated to

My mother

"Ratnamala Manikant Gurave"

&

My father

"Manikant Balvant Gurave"

CERTIFICATE

This is to certify that the thesis titled "**Emulsion Templated Crosslinked Fibrous Membranes via Near-Gel Resin Electrospinning"**, being submitted by **Pramod Manikant Gurave** to the Indian Institute of Technology Delhi for the award of the degree of **Doctor of Philosophy**, is a record of bonafide research work carried out by him. He has worked under my guidance and supervision and fulfilled the requirements for submission of the thesis which has attained the standard required for a Ph.D. degree of this Institute.

The results contained in this thesis have not been submitted, in part or in full, to any other university or institute for the award of any degree or diploma.

Prof. Rajiv K. Srivastava
Department of Textile and Fibre Engineering
Indian Institute of Technology Delhi
New Delhi - 110016, India

Date: 31.07.2024

Place: New Delhi

ACKNOWLEDGMENTS

First and foremost, I would like to express my deep gratitude from the bottom of my heart to my supervisor Prof. Rajiv K. Srivastava for providing me with the opportunity to pursue my PhD under his excellent mentorship. His expertise, insights, and patience have been instrumental in shaping my research and propelling me forward. His expertness in polymer chemistry and electrospinning was invaluable to me throughout the research process, particularly in synthesizing crosslinked fibers using the near-gel resin electrospinning method. He cultivated a work environment devoid of stress within a highly established facility and extended generous support to grow at professional and personal fronts.

I would like to thank Prof. Bhanu Nandan for allowing me to utilize laboratory facilities, especially electrospinning instruments, and providing insights timely.

I extend my sincere appreciation to SRC members, Prof. Ashwini Kumar Agrawal, Prof. Mangala Joshi, and Prof. Selvarajan Nagendran, for their valuable feedback, constructive criticism, and encouragement. Your willingness to share your knowledge has significantly enhanced the quality of my work.

I take this opportunity to first thank The Department of Textile and Fiber Engineering (formerly, Department of Textile Technology), IIT Delhi, and the present and former Heads of the department -Prof. Ramasamy Alagirusamy, Prof. R. S. Rengasamy, Prof. Ashwini Kumar Agrawal, Prof. B. K. Behera and Prof. Rabisankar Chattopadhyay for continuously upgrading the department with advanced research facilities and improved infrastructure, which brings motivation to all the members of the Department and IIT Delhi family.

All the faculty members and supporting staff of the Department are highly thankful for their motivating support. Special thanks to Mr. Rajinder Khattar, Mr. D. Kala, Mr. Amarjeet, and Mr. Rohit Chikara from Fibre Science Laboratory. The enthusiastic support from the members of the Department's- Office, Store and various Laboratories is also acknowledged.

I am highly grateful to the members of Central Research Facility, Nano Research Facility and SMITA Lab of IIT Delhi for their on-time support in analysis of samples. The support provided by Mr. Shivkumar Solanki, Ms. Ashtha Sharma, and Mr. Akshey Kaushal is especially acknowledged for analyzing my samples through electron microscopy.

The special gratitude toward the Government of India, Ministry of Education and ANRF SERB-DST for granting me OVDF fellowship to explore the research at University of Alberta, Canada. I would like to express my gratitude to Prof. Mohtada Sadrzadeh for extending the hands of research collaboration and continual support during the fellowship.

It gave me immense pleasure while working with my institute mates who are not only good colleagues but good friends as well. The all-round support from Dr. Sajan Singh, Dr. Umesh Marathe, Dr. Anilkumar Yadav, Dr. Avinash Raulo, Kaustubh Thakur, Dr. Prakash Khude, Dr. Jitendra Narayan Panda, Dr. Rahul Gadkari, Aashish Joshi, Dr. Vijay Goud, Dr. Sanchayan, Dr. Hardeep Singh, and Dr. Biswajit Samir De is much appreciated.

My sincere gratitude is extended toward my present and former lab mates and seniors, Shweta, Dr. Sumana Bandyopadhyay, Dheeraj Kumar, Sweety Rani, Advitiya Kumar, Sagnik Ghosh, Sachidananda Mohapatra, Anil Yadav, Meenal Agrawal, Dr. Jit Pal, Dr. Surabhi Singh, Dr. Prashansa Dalal, Dr. Sadiya Anjum, Dr. Deepika Malpani, Dr. Labeesh, Dr. Ashish Singh, Ekta Vashishth, Vanshika, Arvind, Rosemery, and Pushpal.

A special thanks to my mentees, Smriti Mishra, Sagar Kumar, Shubhang Dubey, Mayank Guvera, Akash Mishra, Dayanand Shelake, and Rohit Vishwakarma.

I extend my heartfelt gratitude to Prof. Bhuvanesh Gupta, supervisor during my master's program, for imparting invaluable insights into polymer chemistry and functional materials.

I am grateful to Prof. Swapan Kumar Laga, Prof. S. R. Eklahre, Prof. Shrirang Chinta, Prof. A. I. Wasif all from DKTES' TEI, Ichalkaranji and Prof. V. D. Gotmare from VJTI Mumbai for inculcating critical thinking and good lab practices in me.s

I am thankful to my friends including, Shivam Kapil, Sahil Mehta, Vivekanand Shinde, Rohit Nemishte, Pooja Kaushik, Yashdeep Sharma, Kashmira Ghone, Akash Jadhav, Anjali Shinde, Arvind Kumar, Shalini Singh, Md Mizanul, Farah, Kapil Gangwar, Kundan Suman, Sagar Dhanuskar, Shubham Kumar, Shashank Chauhan, Shivam Gupta for spending quality time during the journey.

I want to extend my deepest gratitude toward my father Mr. Manikant Balvant Gurave and my mother Mrs. Ratnamala Manikant Gurave for their unwavering support, encouragement, and love that have been pillars of strength throughout every twist and turn of my journey.

Above all, I humbly express my gratitude and reverence to the Divine God for infusing my life with positive energy and blessings.!

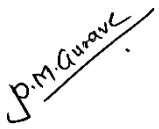

PRAMOD MANIKANT GURAVE

ABSTRACT

Fibers have become essential to human civilization, starting with basic usage to advanced applications. The advancements in textile and polymer science led to the production of various forms of fibers such as yarns, fabrics, nonwovens, and three-dimensional spacer fabrics. Since decades, there has been a surge in interest in producing ultra-thin, one-dimensional structures of fibers, called as nanofiber. The nanofibrous material offers excellent properties such as high aspect ratio, interconnected porosity, flexibility, better mass transport, and enhanced surface area to volume ratio. Technologists have developed various techniques to produce nanofibers from natural and synthetic sources. Among them, electrospinning is the most facile and proven platform to produce transdisciplinary engineered fibrous materials. These nanofibers can then be combined to create advanced two- and three-dimensional structures, like membranes, nonwovens, foams, and aerogels etc. Electrospun fibers face constraints for scalability as the electrospinning process demands preformed polymer with high utilization of hazardous organic solvent for the dissolution of synthetic polymers, which lead to environmental concerns. Moreover, electrospun fibrous materials exhibit poor dimensional stability, against organic solvents at elevated temperature, and mechanical properties which restrict its utilization in real field applications. Crosslinked fibrous materials offer excellent dimensional stability and thermal resistance along with a wide range of applications in sorption, filtration, purification, and catalysis. Direct electrospinning of crosslinked polymers is not viable due to its restricted solubility in solvents. Previous reports highlight the adoption of post-electrospinning crosslinking techniques to produce crosslinked fibrous materials. Very limited options are available for post-crosslinking of electrospun fibers, additionally, this makes the whole process multi-steps and there is no control over morphology of fibers.

Very few reports are available on *in-situ* crosslinking of fibers during electrospinning process. The direct fabrication of crosslinked fibers from their monomeric form is scantly reported in literature. Thus, there is an immense need and research prospects to generate robust electrospun fibrous materials from sustainably electrospinning techniques for real field applications.

In this study, we demonstrated and developed near-gel resin (nGR) electrospinning, through which crosslinked electrospun fibers were produced directly from styrene based monomeric mixtures. The mixture of styrene and divinylbenzene was polymerized using free radical polymerization under non-inert conditions until reaching the gel point, thereby forming a flowable resin. Subsequently, the resin was electrospun in various forms such as bulk, solution, or emulsion to directly produce crosslinked fibers. The effect of variation in crosslinking density on fiber morphology was evaluated. The challenges associated with nGR bulk and solution electrospinning in achieving high crosslinking density were overcome by emulsion electrospinning technique where crosslinked fibers up to 60% theoretical crosslink density were fabricated. As emulsion electrospinning has been referred to as green electrospinning, it minimized the use of organic solvent and promoted successful production of crosslinked polystyrene-based nanofibers in presence of polyvinyl alcohol (PVA). The crosslinked fibers with core-sheath morphology were obtained through precisely optimized parameters affecting emulsion electrospinning, such as template polymer concentration, emulsifier nature and concentration, volume of dispersed phase, and reaction conditions. Through nGR emulsion electrospinning, three generations of nanofibrous membranes were produced, namely, dual crosslinked membrane, silica composite membrane and metal organic frameworks (MOF) decorated nanofibrous membrane. Dual crosslinked fibrous membranes

showed selective wettability toward oil and water as they were composed of fully crosslinked core-sheath fibers. Silica composite membrane was produced via forming Pickering nGR emulsion where silica nanoparticles were used as Pickering stabilizer for producing stable nGR emulsion as well as functional moieties to improve wettability of nanofibrous membrane. Fibrous membranes were enriched with MOF content to create multifunctional MOF-decorated membranes. The prepared membranes were tested as a separation membrane toward various oil/water mixtures and emulsions. All the membrane were thoroughly characterized to evaluate their wettability behavior, anti-fouling nature and oil sorption capacity. Overall, nGR electrospinning technique developed in this work paved a new and unique way to prepare polystyrene based crosslinked electrospun fibers and can be explored for other polymeric systems to produce nanofibrous membranes for advanced applications.

सारांश

रेशे मानव सभ्यता के लिए अत्यावश्यक बन गए हैं, बुनियादी उपयोग से लेकर उन्नत अनुप्रयोगों तक। वस्त्र और बहुलक विज्ञान में प्रगति ने रेशों के विभिन्न रूपों जैसे सूत, कपड़े, गैर-बुने हुए कपड़े, और त्रिआयामी स्पेसर कपड़ों के उत्पादन की ओर अग्रसर किया। दशकों से, रेशों की अत्यंत पतली, एक-आयामी संरचनाओं, जिन्हें नैनोफाइबर कहा जाता है, के उत्पादन में रुचि बढ़ी है। नैनोफाइबर सामग्री उत्कृष्ट गुण प्रदान करती है जैसे उच्च पहलू अनुपात, परस्पर जुड़ी हुई छिद्रता, लचीलापन, बेहतर द्रव्यमान परिवहन, और आयतन के अनुपात में वर्धित सतह क्षेत्र। तकनीकीविदों ने प्राकृतिक और कृत्रिम स्रोतों से नैनोफाइबर का उत्पादन करने के लिए विभिन्न तकनीकें विकसित की हैं। इनमें से, इलेक्ट्रोस्पिनिंग अंतःविषयक इंजीनियर्ड रेशेदार सामग्रियों का उत्पादन करने के लिए सबसे सरल और सिद्ध मंच है। इन नैनोफाइबरों को फिर उन्नत द्विआयामी और त्रिआयामी संरचनाओं, जैसे झिल्लियों, गैर-बुने हुए कपड़ों, फोम, और एयरोजेल आदि बनाने के लिए संयोजित किया जा सकता है। इलेक्ट्रोस्पन फाइबर मापनीयता की बाधाओं का सामना करते हैं क्योंकि इलेक्ट्रोस्पिनिंग प्रक्रिया पूर्व-निर्मित बहुलक की मांग करती है, जिसमें कृत्रिम बहुलकों के विलयन के लिए खतरनाक कार्बनिक विलायकों का उच्च उपयोग होता है, जो पर्यावरणीय चिंताओं को जन्म देता है। इसके अलावा, इलेक्ट्रोस्पन रेशेदार सामग्रियाँ उच्च तापमान पर कार्बनिक विलायकों के प्रति खराब आयामी स्थिरता और यांत्रिक गुणों का प्रदर्शन करती हैं, जो वास्तविक क्षेत्र अनुप्रयोगों में इसके उपयोग को सीमित करता है। क्रॉसलिंक्ड रेशेदार सामग्रियाँ उत्कृष्ट आयामी स्थिरता और तापीय प्रतिरोध के साथ-साथ अवशोषण, छनन, शुद्धिकरण, और उत्प्रेरण में व्यापक अनुप्रयोगों की पेशकश करती हैं। क्रॉसलिंक्ड बहुलकों का सीधा इलेक्ट्रोस्पिनिंग विलायकों में इसकी सीमित घुलनशीलता के कारण व्यवहार्य नहीं है। पिछले प्रतिवेदन क्रॉसलिंक्ड रेशेदार सामग्रियों का उत्पादन करने के लिए पोस्ट-इलेक्ट्रोस्पिनिंग क्रॉसलिंकिंग तकनीकों के अपनाने पर प्रकाश डालते हैं। इलेक्ट्रोस्पन फाइबरों के पोस्ट-क्रॉसलिंकिंग के लिए बहुत सीमित विकल्प उपलब्ध हैं, इसके अतिरिक्त, यह पूरी प्रक्रिया को बहु-चरणीय बना देता है और फाइबरों की आकृति पर कोई नियंत्रण नहीं रहता।

इलेक्ट्रोस्पिनिंग प्रक्रिया के दौरान फाइबरों के इन-सीटू क्रॉसलिंकिंग पर बहुत कम रिपोर्ट उपलब्ध हैं। उनके मोनोमेरिक रूप से सीधे क्रॉसलिंक्ड फाइबरों का निर्माण साहित्य में बहुत कम रिपोर्ट किया गया है। इस प्रकार, वास्तविक क्षेत्र अनुप्रयोगों के लिए स्थायी इलेक्ट्रोस्पिनिंग तकनीकों से मजबूत इलेक्ट्रोस्पन रेशेदार सामग्रियों को उत्पन्न करने की अत्यधिक आवश्यकता और अनुसंधान संभावनाएं हैं।

इस अध्ययन में, हमने नियर-जेल रेजिन (nGR) इलेक्ट्रोस्पिनिंग का प्रदर्शन और विकास किया, जिसके माध्यम से स्टाइरीन आधारित मोनोमेरिक मिश्रणों से सीधे क्रॉसलिंक्ड इलेक्ट्रोस्पन फाइबर उत्पादित किए गए। स्टाइरीन और डाइविनाइलबेंजीन के मिश्रण को गैर-निष्क्रिय परिस्थितियों में मुक्त मूलक बहुलकीकरण का उपयोग करके जेल बिंदु तक पहुंचने तक बहुलकीकृत किया गया, जिससे एक प्रवाहशील रेजिन बना। तत्पश्चात, रेजिन को विभिन्न रूपों जैसे थोक, घोल, या इमल्शन में इलेक्ट्रोस्पन किया गया ताकि सीधे क्रॉसलिंक्ड फाइबर उत्पादित किए जा सकें। फाइबर आकृति पर क्रॉसलिंकिंग घनत्व में परिवर्तन के प्रभाव का मूल्यांकन किया गया। उच्च क्रॉसलिंकिंग घनत्व प्राप्त करने में nGR थोक और घोल इलेक्ट्रोस्पिनिंग से जुड़ी चुनौतियों को इमल्शन इलेक्ट्रोस्पिनिंग तकनीक द्वारा दूर किया गया, जहां 60% तक के सैद्धांतिक क्रॉसलिंक घनत्व वाले क्रॉसलिंक्ड फाइबर निर्मित किए गए। चूंकि इमल्शन इलेक्ट्रोस्पिनिंग को हरित इलेक्ट्रोस्पिनिंग के रूप में संदर्भित किया गया है, इसने कार्बनिक विलायक के उपयोग को कम किया और पॉलीविनाइल अल्कोहल (PVA) की उपस्थिति में क्रॉसलिंक्ड पॉलीस्टाइरीन-आधारित नैनोफाइबर के सफल उत्पादन को बढ़ावा दिया। कोर-शीथ आकृति वाले क्रॉसलिंक्ड फाइबर इमल्शन इलेक्ट्रोस्पिनिंग को प्रभावित करने वाले सटीक रूप से अनुकूलित मापदंडों के माध्यम से प्राप्त किए गए, जैसे टेम्पलेट बहुलक सांद्रता, इमल्सीफायर प्रकृति और सांद्रता, फैली हुई चरण की मात्रा, और प्रतिक्रिया की स्थितियां। nGR इमल्शन इलेक्ट्रोस्पिनिंग के माध्यम से, नैनोफाइबर झिल्लियों की तीन पीढ़ियां उत्पादित की गईं, अर्थात्, द्विगुणित क्रॉसलिंक्ड झिल्ली, सिलिका कंपोजिट झिल्ली और धातु कार्बनिक फ्रेमवर्क (MOF) सजाई गई नैनोफाइबर झिल्ली। द्विगुणित क्रॉसलिंक्ड फाइबर झिल्लियों ने तेल और पानी के प्रति चयनात्मक गीलेपन दिखाया क्योंकि वे पूरी

तरह से क्रॉसलिंक्ड कोर-शीथ फाइबर से बनी थीं। सिलिका कंपोजिट झिल्ली पिकरिंग nGR इमल्शन बनाकर उत्पादित की गई थी जहां सिलिका नैनोकणों का उपयोग स्थिर nGR इमल्शन उत्पादन के लिए पिकरिंग स्थिरक के रूप में किया गया था और साथ ही नैनोफाइबर झिल्ली की गीलेपन में सुधार करने के लिए कार्यात्मक अणुओं के रूप में भी किया गया था। फाइबर झिल्लियों को MOF सामग्री से समृद्ध किया गया ताकि बहुक्रियात्मक MOF-सजाई गई झिल्लियां बनाई जा सकें। तैयार की गई झिल्लियों का परीक्षण विभिन्न तेल/पानी मिश्रणों और इमल्शनों के प्रति पृथक्करण झिल्ली के रूप में किया गया। सभी झिल्लियों का उनके गीलेपन व्यवहार, गंदगी-विरोधी प्रकृति और तेल अवशोषण क्षमता का मूल्यांकन करने के लिए पूरी तरह से चरित्र-चित्रण किया गया। कुल मिलाकर, इस कार्य में विकसित nGR इलेक्ट्रोस्पिनिंग तकनीक ने पॉलीस्टाइरीन आधारित क्रॉसलिंक्ड इलेक्ट्रोस्पन फाइबर तैयार करने के लिए एक नया और अनूठा तरीका प्रस्तुत किया और इसका अन्वेषण अन्य बहुलक प्रणालियों के लिए उन्नत अनुप्रयोगों हेतु नैनोफाइबर झिल्लियों का उत्पादन करने के लिए किया जा सकता है।

Table of Contents

Content			Page number
Certificate			i
Acknowledgements			ii
Abstract			iv
सारांश			vii
Table of Contents			x
List of Figures and Schemes			xv
List of Tables			xx
List of Symbols			xxi
List of Abbreviations			xxiii
Chapter 1	**Introduction and Motivation**		1-17
1.1	Introduction		2
1.2	Motivation		7
1.3	Goal of the work		9
1.4	Thesis organization		10
Chapter 2	**Theoretical Background and Literature Overview**		18-59
2.1	Fiber Manufacturing Techniques		19
	2.1.1	Solution wet spinning	20
	2.1.2	Melt spinning	21
	2.1.3	Microfluidic extrusion	22
	2.1.4	Self assembly	22
	2.1.5	Blow spinning	23

2.1.6 Direct writing 23

2.1.7 Electrospinning 24

2.2 Electrospinning types and methods 25

2.2.1 Melt electrospinning 26

2.2.2 Solution electrospinning 27

2.2.3 Co-axial electrospinning 28

2.2.4 Needleless electrospinning 29

2.3 Green electrospinning 30

2.3.1 Reactive electrospinning 31

2.3.2 Emulsion electrospinning 37

2.4 Polystyrene based crosslinked nanofibers 43

2.5 Electrospun nanofibrous membrane 45

2.6 Summary 47

2.7 Objectives 48

Chapter 3 Experimental Techniques 60-72

3.1 Introduction 61

3.2 Materials 61

3.3 Methods 62

3.3.1 Preparation of near-gel resin (nGR) 62

3.3.2 Preparation of near-gel resin (nGR) emulsion 62

3.3.3 Electrospinning and fabrication of nanofibrous membranes 63

3.4 Characterization 64

3.4.1 Stability of nGR emulsion 64

3.4.2 Proton nuclear resonance spectroscopy (^{1}H-NMR) 64

3.4.3 Fourier transform infrared spectroscopy (FTIR) 64
3.4.4 Differential scanning calorimetry (DSC) 64
3.4.5 Optical microscopy 65
3.4.6 Scanning electron microscopy (SEM) 65
3.4.7 Energy dispersive X-ray scattering (EDS) 65
3.4.8 Transmission electron microscopy (TEM) 66
3.4.9 Confocal microscopy 66
3.4.10 Atomic force microscopy (AFM) 66
3.4.11 Pore size 66
3.4.12 Porosity 67
3.4.13 Contact angle analysis 67
3.4.14 Mechanical strength 68
3.4.15 Wide angle X-ray diffraction (WAXD) 68
3.4.16 Gel content 68
3.4.17 Oil adsorption capacity 68
3.4.18 Oil/water stratified mixture separation 69
3.4.19 Oil-in-water (O/W) emulsion separation 70
3.4.20 Ultraviolet (UV)-visible spectroscopy 70

Chapter 4 Near-gel Resin (nGR) Emulsion Electrospinning 73-111

4.1 Introduction 74

4.2 Experimental 76

4.2.1 Materials 76
4.2.2 Synthesis of near-gel resin (nGR) 77
4.2.3 Preparation of near-gel resin (nGR) emulsion 77

	4.2.4	Electrospinning of nGR and its emulsion	78
	4.2.5	Characterization	78
4.3	Results and Discussion		81
4.4	Conclusions		107
Chapter 5	**Emulsion Templated Dual Crosslinked Nanofibrous Membrane**		112-143
5.1	Introduction		113
5.2	Experimental		116
	5.2.1	Materials	116
	5.2.2	Core crosslinked membrane	117
	5.2.3	Fabrication of dual crosslinked membranes	117
	5.2.4	Characterization	118
5.3	Results and Discussion		123
5.4	Conclusions		140
Chapter 6	**Pickering Emulsion Templated Nanocomposite Membrane**		144-178
6.1	Introduction		145
6.2	Experimental		148
	6.2.1	Materials	148
	6.2.2	Pickering emulsion synthesis	149
	6.2.3	Fabrication of nanocomposite membrane	149
	6.2.4.	Characterization	150
6.3	Results and Discussion		154
6.4	Conclusions		173
Chapter 7	**MOF Decorated Multifunctional Nanofibrous Membrane**		179-210
7.1	Introduction		180

7.2	Experimental		182
	7.2.1	Materials	182
	7.2.2	Fabrication of dual crosslinked nanofibrous membrane (DCNM)	182
	7.2.3	Preparation of ZIF-8 decorated DCNM (ZIF-8@DCNM)	183
	7.2.4	Characterization	183
7.3	Results and Discussion		187
7.4	Conclusions		206
Chapter 8	**Conclusions and Future Outlook**		211-214
9.1	Conclusions		212
9.2	Future Outlook		214
	Curriculum-Vitae		215-217

List of Figures and Schemes

Figure number	Figure-Caption	Page number
2.1	Schematic representation of various advanced fiber manufacturing techniques.	20
2.2	Schematic presentation of basic electrospinning with types of electrospinning.	26
2.3	Process of emulsion electrospinning and fiber formation.	38
2.4	Water stress mapping of countries in the world.	46
3.1	UV-visible absorbance spectra of extracts of emulsions of different oil concentration.	72
4.1	Preparation of nGR electrospinning solution.	83
4.2	SEM images of electrospun samples of BS1 and BS2 where polymerization time was 2 h and 4 h, respectively.	85
4.3	1H NMR spectra of BS2 nGR and fibers.	85
4.4	SEM images of electrospun fibers from nGR ([M]/[I]=500) of BS3, BS4, BS5, at as-spun and thermal treated state.	86
4.5	Process for the fabrication of crosslinked polystyrene fibrous membrane through nGR emulsion electrospinning.	88
4.6	Optical images of electrospun fibers (EB1 to EB5) using nGR emulsions with varying PVA concentration of 3 to 7 %, respectively.	91
4.7	SEM images of as-spun and thermal treated electrospun fibers with varying ϕ_d.	93
4.8	Optical morphology of nGR emulsions and respective electrospun fibers at varying SDS concentration of 1% and 2 %.	94
4.9	confocal and TEM images electrospun fibers prepared from nGR emulsion with reaction time of 0.75 h (EB4), 2 h (EB12) and 2.5 h (EB11).	96
4.10	Viscosity profile of emulsions produced using SDS (EB12 to EB14) and Brij-58 (EB15 to EB17).	98
4.11	Optical images of nGR emulsions of EB12-EB17 with its droplet size distribution.	99

4.12	SEM micrographs of the as-spun electrospun fibers obtained from emulsions stabilized with SDS (EB12, EB13, EB14) and Brij-58 (EB15, EB16, and EB17) with varying X_c of 40, 50, and 60%, respectively.	100
4.13	Schematic representing the proposed mechanism for fiber formation in nGR emulsion electrospinning.	101
4.14	Optical images (A, B) of emulsions stabilized with SDS and Brij-58 [EB12 and EB15] and related fiber morphology through confocal images (C, D) and TEM micrographs (E, F), respectively.	103
4.15	TEM micrographs of fiber morphology of EB13, EB14, EB16, EB17.	104
4.16	Gel content of electrospun fibrous crosslinked membrane.	106
4.17	Oil adsorption of crosslinked electrospun membrane along with digital image of swollen of EB12 membrane in toluene.	107
5.1	SEM images at (A) 10Kx, (A') 30Kx with (B) fiber diameter distribution. (C) TEM image of core crosslinked nanofibers of CM1 sample.	125
5.2	(A) SEM images, (B) FTIR spectra and (C) water adsorption capacity hydration ability of dual crosslinked membranes.	126
5.3	(A, B) SEM image showing surface of DCM2 membrane along with fiber diameter distribution, (C) SEM image showing cross-sectional view of membrane, (D) TEM image of single nanofiber, (E) Porosity and pore size of DCM2 membrane and (F) digital picture showing solubility of membranes in water.	128
5.4	TEM images of core crosslinked fibres dispersed in water when CM1 exposed to water medium.	129
5.5	SEM images of DCM2 membrane after prolonged soaking in (A) water and (B) toluene for 3 months.	129
5.6	(A) Digital photograph of dual crosslinked nanofibrous membrane of sample DCM2. (B) digital photograph showing wettability of membranes towards water (yellow dyed) and oil (blue dyed). (C, D) images of water and oil spreading on membranes in air. (E) underwater oil contact angles towards DCM2 membrane. (F1-4) selective wettability assessment of nanofibers through confocal microscopy.	130
5.7	SEM and TEM images of DCM6 (A, A') and DCM7 (B, B') membrane, respectively. Gel content of dual crosslinked membranes (C).	132
5.8	(A) Comparison of adsorption capacity towards different oils by the membranes with varying core Xc. (B) cyclic variation of adsorption capacity toward toluene by DCM2 membrane.	133

5.9	(A) Digital image and (B) SEM image of DCM2 membrane after cyclic oil adsorption.	134
5.10	(A) Pictorial illustration of oil/water mixture separation experiment conducted under 600 mbar vacuum. (B) separation performance of DCM2 membranesfor four oil/water mixtures. (C, D) separation flux and efficiency of four types of oil/water mixtures towards multiple separation cycles.	135
5.11	(A, B) Optical images of n-hexane-in-water emulsions (SE and NE) and corresponding filtrate images and UV-visible spectrum. (C) separation fluxes and efficiencies for different SE and NE emulsions separated under 600 mbar vacuum by DCM2 membranes. (D) separation flux and efficiency for n-hexane-in-water emulsions (SE and NE) passed through DCM6 and DCM7 membranes.	137
5.12	Optical images of SE and NE emulsions and corresponding filtrate optical images and UV-visible spectra.	138
5.13	Cyclic performance for (A) separation flux and (B) separation efficiency of DCM2 matrices towards n-hexane emulsions.	139
6.1	TEM image of SiO_2 nanoparticles.	155
6.2	Digital Images of Pickering emulsions with SiO_2 content 0.5%, 1%, 3% and 5% showing stabilizing behavior.	156
6.3	SEM images at 2Kx and 20Kx magnification with corresponding fibre diameter distribution of membranes SPEM1 (A, B, C), SPEM3 (D, E, F) and SPEM5 (H, I, J) respectively. The insert circles showing presence of SiO_2 particles over the surface.	159
6.4	WCA and UWOCA of membranes with variation in SiO_2 content.	160
6.5	(A) Digital image of SPEM3 membrane, (B) HRTEM image of single fiber, (C) fiber image at high magnification, (D) EDX mapping images of SPEM3 membrane. Red, cyan, green dots indicate signals for carbon (C), oxygen (O) and silicon (Si), respectively. (E) The element composition of SPEM3 membrane surface.	161
6.6	FTIR spectra for SPEM3 membrane.	162
6.7	(A) The AFM image and (B) pore size, porosity of SPEM3 membrane.	163
6.8	Wetting characteristics of SPEM3 membrane.	165
6.9	(A) Oil adsorption capacity of SPEM3 membrane towards oils. (B) Cyclic adsorption performance of SPEM3 membrane towards toluene.	166

6.10	(A) Oil-water mixture separation performance of SPEM3 membrane towards various oils. (B) Multiple cycles separation performance towards n-hexane/water mixture.	167
6.11	Multiple cycles separation performance of SPEM3 membrane towards (A) petrol/water, (B) toluene/water and (C) silicone oil/water mixture.	168
6.12	(A) Pictorial presentation of separation process with filter assembly. (B, C) Optical microscopic images of n-hexane emulsions (NE, SE) and its filtrates, respectively. Separation performance of SPEM3 membrane towards NE (D) and SE emulsions (E) of different oils.	169
6.13	(A) Multiple cycle separation performance towards n-hexane SE emulsion. (B) Schematic illustration of separation process mechanism for emulsion.	171
6.14	SEM images showing structural stability of SPEM3 membrane at 80°C.	172
6.15	(A) Separation performance of membrane towards hot toluene-in-water SE emulsion. (B) Underwater oil contact angle for SPEM3 membrane towards toluene at (A) 60°C and (B) 80°C.	172
7.1	FESEM images of membrane at low and high magnification with fiber diameter distribution 10ZIF-8DCNM (A, A1, A2), 30ZIF-8DCNM (B, B1, B2) and 60ZIF-8DCNM (C, C1, C2) membranes, respectively.	189
7.2	Graph showing effect of ZIF-8 loading on the wettability of membranes through WCA and UWOCA. n-Hexane was used as model oil for measuring UWOCA of the membranes.	190
7.3	The effect of ZIF-8 loading on the separation performance toward NE and SE emulsions.	191
7.4	FESEM image of DCNM (A) and 30ZIF-8@DCNM membrane (B). Inset showing FESEM images at high magnification. EDX elemental mapping of 30ZIF- 8@DCNM membrane (C). AFM images of DCNM and 30ZIF-8@DCNM (D, E), respectively.	193
7.5	TEM image of single nanofiber of 30ZIF-8@DCNM membrane (A). XRD pattern (B) and FTIR spectra (C) of ZIF-8 and of 30ZIF-8@DCNM membrane, respectively.	194
7.6	Dynamic wetting of 30ZIF-8@DCNM membrane toward water and oil, respectively (A, B). Digital images showing anti-oil adhesion behaviour of membrane (C). UWOCAs of the membrane (D). Digital image of the prepared membrane with its cross-sectional view SEM.	196
7.7	Digital images (A, A1) of n-hexane SE emulsion with its corresponding permeate. Graph showing comparative performance of the membranes	198

	with permeation flux (B) and separation efficiency (C) toward various SE emulsions.	
7.8	Graphs showing comparative performance of the membranes with permeation flux and efficiency toward various NE emulsions.	199
7.9	Study on cyclic separation test with SE emulsion of toluene and n-hexane (A, B). Performance test under different conditions of SE emulsions of toluene and n-hexane (C, D).	200
7.10	SEM images showing structural stability of 30ZIF-8@DCNM membrane after cyclic separation in toluene SE emulsion (A), after evaluating corrosion resistance in 4M HCl (B) and thermal resistance at 80° C (C).	201
7.11	Schematic presentation of emulsion separation mechanism of the developed ZIF-8@DCNM membrane.	202
7.12	Graph showing Cu2+ and Pb+2 ion rejection for DCNM and 30ZIF-8@DCNM membranes during toluene-in-water emulsion separation at 100 ppb ion concentration. Elemental mapping images with content analysis of the membrane after separation of toluene-in-water emulsion containing Cu2+ and Pb2+.	203
7.13	Sorption capacity of various membranes toward various oils at equilibrium (A). Comparative sorption kinetics of DCNM and 60ZIF-8@DCNM membranes for toluene (B). Cyclic sorption test (C).	204

Scheme number	**Scheme-Caption**	**Page number**
5.1	Schematic showing fabrication of dual crosslinked membranes.	124
5.2	Reaction mechanism of crosslinking in core and sheath domain of fibre.	124
6.1	Schematic representing the process for producing SiO2-Pickering emulsion templated nanocomposite membrane (SPEM).	157
6.2	Process of fibre formation through nGR Pickering emulsion.	158

List of Tables

Table number	Table-Caption	Page number
2.1	Reactive electrospinning and method of crosslinking.	34
2.2	electrospun fibers developed through O/W emulsion electrospinning.	40
2.3	Electrospun fibers developed through O/W emulsion electrospinning.	41
2.4	Crosslinked electrospun fibers developed through emulsion electrospinning.	43
4.1	Parameters and characteristics of nGR and its electrospinning.	82
4.2	Parameters and characteristics of nGR emulsion, and its electrospun fibers.	90
4.3	Mechanical characteristics of SDS-stabilized nGR emulsion electrospun membranes.	105
5.1	Core and dual crosslinked fibrous membranes.	125
5.2	Mechanical characteristics of core and dual crosslinked fibrous membranes.	127
5.3	Characteristics of oils and emulsions used.	136
6.1	Characteristics of oils and emulsions used.	153
6.2	SiO_2 stabilized nGR Pickering emulsions and produced nanocomposite membranes.	155

List of Symbols

s	Second
min	Minute
h	Hour
m	Meter
cm	Centimeter
mm	millimeter
µm	micrometer
nm	Nanometer
cm^{-1}	Centimetre inverse
L	Litre
mL	Millilitre
µL	Microlitre
mL min^{-1}	Millilitre per minute
%	Percentage
ppm	Parts per million
g	Gram
mg	Milligram
mol	Mole
g mol^{-1}	Gram per mole
g cm^{-3}	Gram per cubic centimetre
m^2 g^{-1}	Square meter per gram
J/g	Joule per gram

kHz	Kilohertz
MHz	Megahertz
kV	Kilovolt
°C	Degree Celsius
T_g	Temperature of glass transition
T_m	Temperature of melting
T_c	Temperature of crystallization
H_f	Heat of fusion
H_f^0	Heat of fusion of 100% crystalline poly(ε-caprolactone) sample
H_c	Heat of crystallization
Pa	Pascal
MPa	Mega-Pascal
ρ	Density
N	Newton
L m^{-2} h^{-1}	Litre per square meter per an hour

List of Abbreviations

nGR	Near-gel resin
DCM	Dual crosslinked membrane
DCNM	Dual crosslinked nanofibrous membrane
SPEM	SiO_2-Pickering emulsion-templated nanocomposite membrane
MOF	Metal organic frameworks
ZIF-8	Zeolitic imidazole framework 8
2D	Two-dimensional
3D	Three-dimensional
RT	Room temperature
rpm	Revolution per minute
wt.%	Weight percentage
w.r.t.	With respect to
X_c	Crosslink density
ϕ_d	Volume fraction of dispersed phase
ϕ_c	Volume fraction of continuous phase
W/O	Water-in-oil
PP	Polypropylene
PAN	Polyacrylonitrile
PVDF	Polyvinylidene fluoride
PU	Polyurethane
O/W	Oil-in-water
PLLA	Poly(L-lactic acid)

PDLA	Poly(D,L-lactide)
PVA	Polyvinyl alcohol
PEO	Poly (ethylene oxide)
PCL	Poly(ε-caprolactone)
PEGDMA	Poly(ethylene glycol) dimethacrylate
AA	Acrylic acid
AM	Acrylamide
SMA	Stearyl methacrylate
HEMA	2-Hydroxyethyl methacrylate
GMA	Glycidyl methacrylate
DVB	Divinyl benzene
EGDMA	Ethylene glycol dimethacrylate
SiO_2	silica nanoparticles
DCE	Dichloroethane
$CDCl_3$	Deuterated chloroform
THF	Tetrahydrofuran
DMF	N,N'-Dimethyl formamide
^{1}H-NMR	Proton nuclear magnetic resonance spectroscopy
SEM	Scanning electron microscopy
FE-SEM	Field emission-scanning electron microscopy
TEM	Transmission electron microscopy
WAXD	Wide angle X-ray diffraction
EDS	Energy dispersive X-ray spectroscopy
FTIR	Fourier transform infrared spectroscopy

ATR	Attenuated Total Reflectance
DSC	Differential scanning calorimetry
Cu	Copper
K	Potassium
Hg	Mercury
HCl	Hydrochloric acid